Am J Transl Res 2020;12(10):6160-6169
www.ajtr.org /ISSN:1943-8141/AJTR0114251

Original Article

Biomechanical evaluation of four different posterior instrumentation techniques for single-level transforaminal lumbar interbody fusion: a finite element analysis

Hui-Zhi Guo[1,2], Yong-Chao Tang[2], Dan-Qing Guo[1], De Liang[2], Shun-Cong Zhang[2]

[1]The First Institute of Clinical Medicine, Guangzhou University of Chinese Medicine, Guangzhou, Guangdong, China; [2]Spine Surgery Department, The First Affiliated Hospital of Guangzhou University of Chinese Medicine, Guangzhou, Guangdong, China

Received May 12, 2020; Accepted August 28, 2020; Epub October 15, 2020; Published October 30, 2020

Abstract: This study aims to investigate the fixation strength of unilateral cortical bone trajectory screw fixation (UCBT) and UCBT with contralateral translaminar facet screw fixation (UCBT-TFS) by repeating the verification of three finite element models. Three healthy female models of the lumbosacral spine were constructed. For each of them, four transforaminal lumbar interbody fusion (TLIF) models with the following instruments were created: bilateral traditional trajectory pedicle screw fixation (TT), bilateral cortical bone trajectory screw fixation (CBT), UCBT, and UCBT-TFS. A 150-N compressive load with 10 N/m moments was applied to simulate flexion, extension, lateral bending, and axial rotation. The range of motion (ROM), the stress of the cages, and the stress of the posterior fixations were compared. TT and UCBT-TFS had a similar low ROM compared to the intact models, and CBT showed a higher ROM in lateral bending. UCBT resulted in the highest ROM under all loading conditions, especially in lateral bending (116% and 170% greater than TT in left bending and right bending). UCBT induced a significant increase in the peak stress of cages and instruments, followed by CBT and UCBT-TFS, and the lowest mean values were observed for TT. Among the four different fixation techniques, TT offered the highest fixation strength and lowest implant stress, followed by UCBT-TFS and CBT, while UCBT was the least stable and resulted in increased stress of the screws and cages. UCBT-TFS improved biomechanical stability and appeared to be a less invasive alternative in well-selected patients with single-level TLIF.

Keywords: Cortical bone trajectory, unilateral, translaminar facet screw, transforaminal lumbar interbody fusion, finite element analysis, biomechanical stability

Introduction

With the development of surgical technology and implanted instruments, the number of lumbar fusion surgeries has increased rapidly for the past three decades. Deyo et al. [1] found that the annual number of lumbar fusion operations increased from approximately 61,000 in 1993 to over 450,000 in 2011 (an increase of 600%) in the United States. Pedicle screw fixation, the classic technology to treat spinal degenerative disorders, vertebral deformities, and metastatic tumors, has been applied for more than 60 years since it was first described in 1959 by Boucher [2]. However, several limitations of pedicle screws have also been reported in the literature, including excessive dissection of paraspinal muscles, screw loosening, and instrument failure [3-5].

Based on the modification of the screw track in traditional trajectory pedicle screw (TT), Santoni et al. [6] described a novel cortical bone trajectory (CBT) screw fixation method with approximate pullout strength and mechanical performance compared with TT in 2009. In terms of the screw path, the entry point of CBT is closer to the midline of the spine, and the screw-bone interface is located in the stiffer cortical bone. The in vivo analysis of CBT dem-

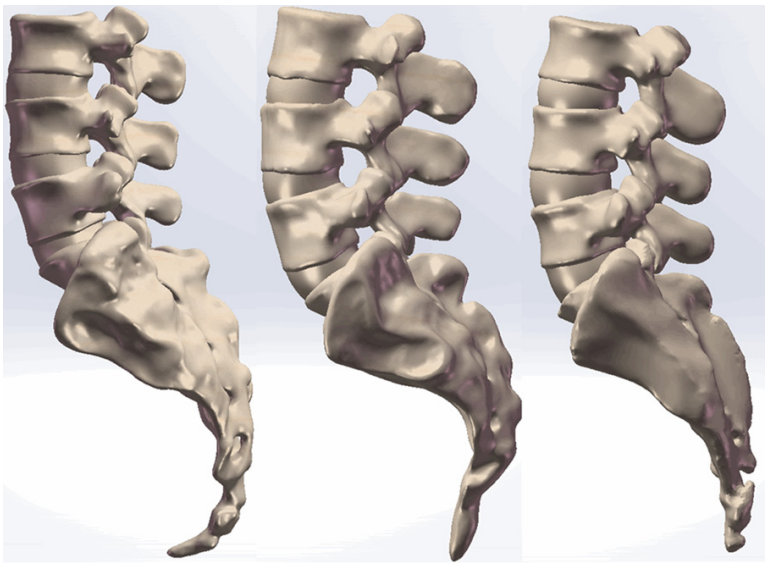

Figure 1. Reconstructions of the intact lumbosacral models of the three female volunteers involved in the present study. Because the analysis of this study did not involve coccyx, the geometry characteristics of the coccyx in patient 3 (right) were simplified.

onstrated a 30% increase in uniaxial yield pullout load [6] and 1.7 times higher torque relative to TT [6, 7]. Therefore, considering the better biomechanical properties of CBT screw fixation, unilateral cortical bone trajectory screw fixation (UCBT) and a combined fixation of UCBT with a contralateral translaminar facet screw (UCBT-TFS) have received increasing attention by spine surgeons as a type of less invasive alternative fixation [8]. However, none of the previous studies evaluated the biomechanical performance of UCBT and UCBT-TFS. This is the first study to investigate the stability of these fixation techniques by repeated testing of three different finite element models.

Materials and methods

Model development of the lumbosacral spine

To improve the reliability and repeatability of the analysis results in this study, finite element (FE) models of different healthy volunteers were constructed for repetitive testing. Two independent spine surgeons were assigned to exclude the spinal deformities of volunteers. Finally, the high-resolution computed tomography data (AQUIRRON 64, Toshiba, Japan, 250 mAs, 120 kV voltage, slice thickness of 0.625 mm) of three healthy adult females were acquired and stored in a hard disk. The average age of the three volunteers was 35 (range 28-41) years old.

Anatomical 3D models of the lower lumbar vertebrae, sacrum, and coccyx were generated using Mimics research 19.0 (Materialize, Leuven, Belgium) (because the analysis of this study did not involve the coccyx, the geometric characteristics of the coccyx in patient 3 were simplified). The intact models were embedded into Geomagic Studio 2013 (3D Systems Corporation, Rock Hill, South Carolina, USA) for further operation, including retriangulation and smoothing of the polygon mesh, making triangles more uniform in size, and generating an NURBS surface on the object. The cancellous bone and posterior bone were generated by offsetting the entire vertebral body. Then, the smoothed models were processed using SolidWorks 2017CAD (SolidWorks Corporation, Concord, MA, USA) to construct the vertebral endplates, annulus fibrosus, nucleus pulposus, and facet cartilage parts.

The bodies of the vertebrae, including cortical bone, cancellous bone, and posterior bone, were set as solid elements. Cancellous bone was covered by a 0.5 mm thick cortical bone [9]. Two cartilaginous endplates with a thickness of 1 mm were attached to the upper and lower surfaces of the cortical bone [10, 11]. The annulus fibrosus was assumed to be a composite of seven crisscrossing fiber layers with an inclination to the transverse plane between 15° and 30° [12]. The fiber content accounted for approximately 19% of the annulus fibrosus, similar to a real annulus [12]. The nucleus pulposus, simulated as a fluid-like and incompressible material, occupied 44% of the disc volume [9]. The breadth of the facet joints was approximately 0.3-0.6 mm according to the natural distance in CT. The parts described above were assembled into intact lumbosacral models (**Figure 1**). The midsagittal diameter (width), transverse diameter (length), and height of the L4/L5 vertebral body were

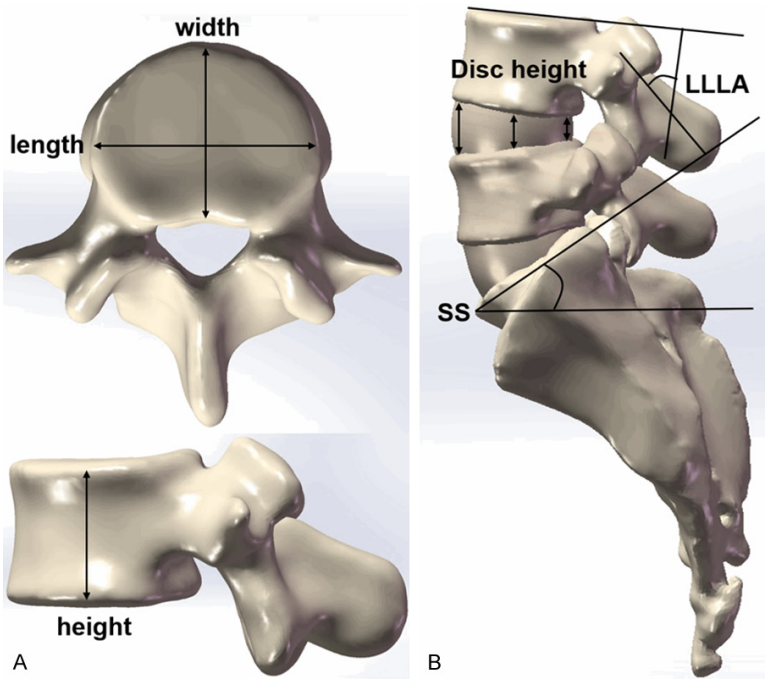

Figure 2. Demonstration of the anatomical measurements. A. Measurements of the vertebral body length, width, and height. B. Measurements of the disc height, lower arc of lumbar lordosis (LLLA), and sacral slope (SS). The disc height at L4/5 was the mean value of the anterior edge, center, and posterior edge of the disc. The LLLA was defined as the angle between the upper endplate of L4 and the endplate of S1. The SS was defined as the angle between the horizontal line and the endplate of S1.

measured by SolidWorks [13]. The height of the vertebral body was defined as the distance between the upper and lower cortical bone. The disc height at L4/5 was the mean value of the anterior edge, center, and posterior edge of the disc [14]. The lower arc of lumbar lordosis (LLLA) was defined as the angle between the upper endplate of L4 and the endplate of S1 [15]. The sacral slope (SS) was defined as the angle between the horizontal line and the endplate of S1 (**Figure 2**) [16]. Finally, the intact lumbosacral models were imported into ANSYS Workbench 17.0 (ANSYS, Ltd., Canonsburg, Pennsylvania, USA) for setting material properties, defining major ligaments, and generating meshes.

Construction of surgical models

Transforaminal lumbar interbody fusion (TLIF) was assumed at the L4-5 level to excise the joint cartilage, the right facet joint, and part of the annulus fibrosus, nucleus, and cartilaginous endplates. The interbody cage was placed obliquely in the middle of the intervertebral space and filled with cancellous bone allograft to simulate the embedded allogeneic bone graft. Then, the TLIF models were applied with four different fixation techniques: (1) bilateral traditional trajectory pedicle screw fixation (TT); (2) bilateral cortical bone trajectory screw fixation (CBT); (3) UCBT; and (4) UCBT-TFS (**Figure 3**). In total, sixteen finite element models were created. In all four fusion models, the cage was placed in the same location. The posterior rods, cage, TT screws, CBT screws, and facet screws were constructed according to our previous report [12]. The posterior rods had a diameter of 5.5 mm; the cage had a length of 24 mm and a height of 12-14 mm (according to the different disc heights of the models); the TT screws had a length of 50 mm and a diameter of 6 mm; the CBT screws had a length of 35 mm and a diameter of 5 mm; and the translaminar facet screw had a length of 45 mm and a diameter of 3.5 mm. The entry point of the cortical bone trajectory was located at the intersection of the lower border of the transverse process and the midline of the superior articular process, inclining 30-45 degrees to the head side and 20 degrees to the lateral side [17]. The entry point of the translaminar facet screw was located at the junction of the lamina-spinous process, and the screw was passed through the left facet joint [18].

Biomechanical analysis

All the FE models were imported into ANSYS Workbench 17.0 for biomechanical testing. The sacroiliac joint was bilaterally fixed with all degrees of moment restricted throughout the whole analysis. To simulate the weight of the body and movement load, a vertical compressive force of 150 N was used on the upper surface of L3, and a 10-N/m moment was applied along the radial direction in flexion, extension, left lateral bending, right lateral bending, left rotation, and right rotation [10, 19]. The mate-

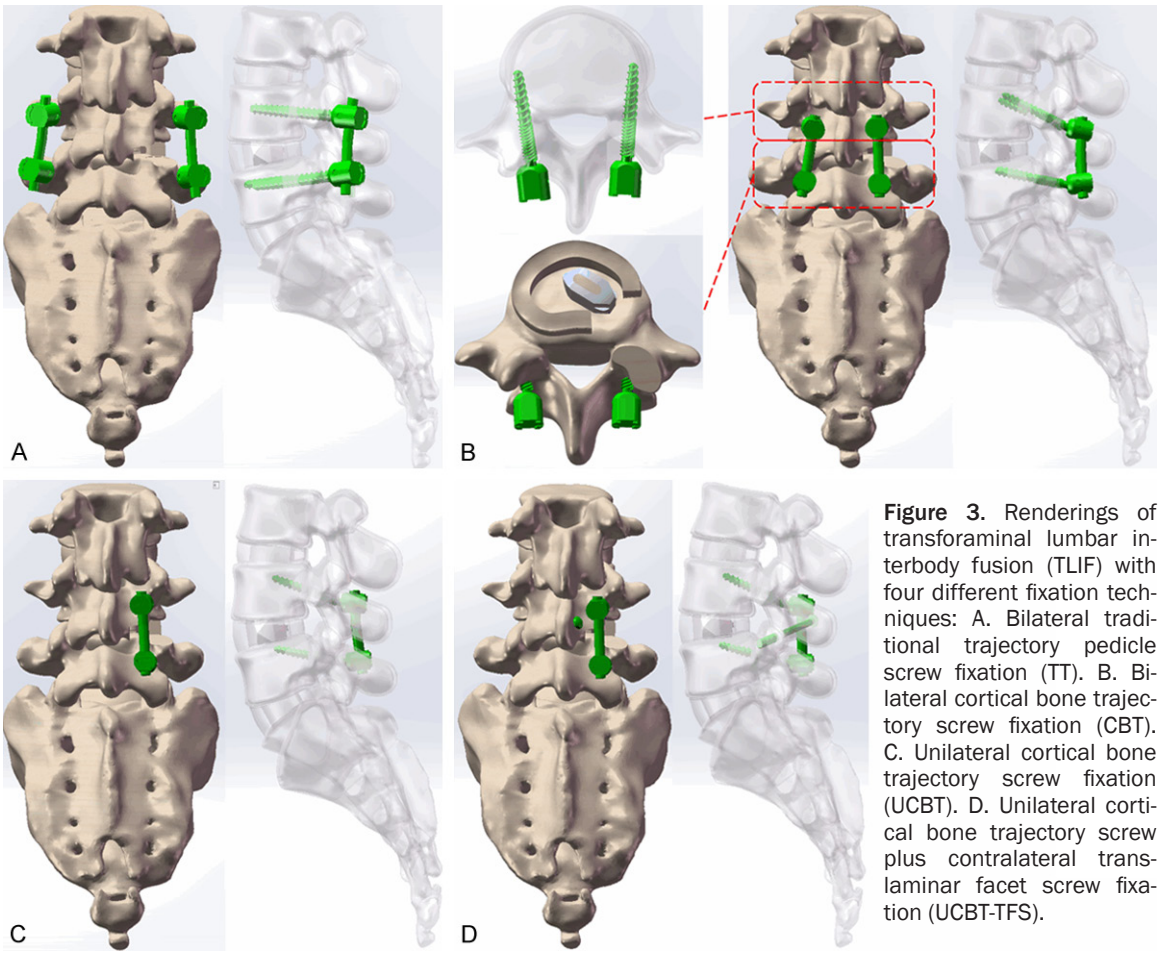

Figure 3. Renderings of transforaminal lumbar interbody fusion (TLIF) with four different fixation techniques: A. Bilateral traditional trajectory pedicle screw fixation (TT). B. Bilateral cortical bone trajectory screw fixation (CBT). C. Unilateral cortical bone trajectory screw fixation (UCBT). D. Unilateral cortical bone trajectory screw plus contralateral translaminar facet screw fixation (UCBT-TFS).

Table 1. Material properties assumed for posterior fixations, bone-graft, and spinal cages

Bodies	Material	Young's Modulus (GPa)	Poisson's Ratio (μ)	References
Posterior fixations	titanium alloy (Ti-6A1-4V)	110	0.28	[21]
Bone graft	cancellous bone	0.1	0.2	[10]
Spinal cage	polyetheretherketone	3.6	0.25	[10]

rial properties were assumed to be isotropic elasticity according to our previous study [20]. The material of the intervertebral bone graft was assumed to the cancellous allograft bone properties [10]. The material of posterior fixations and spinal cage was assumed as titanium alloy and polyetheretherketone (**Table 1**) [10, 21]. The L4-5 disc was degenerated, changing the elastic material properties of the annulus. The ligaments of the spine were simulated using tension-only and nonlinear spring elements. The stiffness of the springs was taken from previous validation experiments on FE models (spring stiffness = (modulus of elasticity × cross-section)/average length) [22, 23]. The stiffness of the anterior longitudinal ligament, posterior longitudinal ligament, ligamentum flavum ligament, supraspinous ligament, interspinous ligament, transverse ligament, and capsular ligament was 8.74 N/mm, 5.83 N/mm, 15.75 N/mm, 15.38 N/mm, 0.19 N/mm, 2.39 N/mm, and 10.85 N/mm, respectively. The contact type of the facet joint was defined as "frictional", and the friction coefficient was set at 0.1. The remaining bodies were defined as the "bonded" mode [11]. The optimum mesh was generated with hexahedral elements (C3D4). The dimension of the joint cartilage mesh was 0.5 mm, while that of the other bodies was 2.0 mm. The ROM, cage

Table 2. Anatomical measurements of three intact models

	Patient 1	Patient 2	Patient 3	Anatomical study	References
L4 width (mm)	36.2	28.9	35.2	33.0±0.4	[13]
L4 length (mm)	50.4	42.3	46.9	43.6±0.5	[13]
L4 height (mm)	26.3	26.0	25.8	25.5±0.3	[13]
L5 width (mm)	34.8	28.2	35.4	34.2±0.3	[13]
L5 length (mm)	52.9	42.3	47.4	44.5±0.4	[13]
L5 height (mm)	25.5	25.8	25.7	25.9±0.3	[13]
Disc height at L4/5 (mm)	7.2	6.3	8.1	8.5±1.6	[14]
Lower arc of lumbar lordosis (°)	24.1	33.2	36.8	28.8±9.9	[15]
Sacral slope (°)	29.8	35.1	34.5	34.4±8.0	[16]

stress, and posterior fixation stress were recorded to make a biomechanical comparison of TLIF with the four fixation techniques.

Results

Morphometric characteristics and sagittal parameters of intact lumbosacral models

The geometrical measurements of vertebral body size and disc height were in the range documented by previous anatomical studies [13, 14]. The measurement of sagittal parameters showed a good match with Chinese asymptomatic adults (**Table 2**) [15, 16]. According to the quantitative comparison, all three lumbosacral models were proven to be suitable for further FE analysis.

Validation of the intact model

The final intact models contained between 630,212 and 958,474 nodes and 393,835 and 521,823 elements. The average ROMs of L3-4 level during flexion, extension, bending, and rotation were 4.13°, 3.65°, 3.57°, and 1.78°, respectively, 5.21°, 3.84°, 3.54°, and 2.16° at the L4-5 level, respectively, and 5.90°, 3.51°, 2.70°, and 1.51° at the L5-S1 level, respectively. The comparison between our results and the reported data in the three models showed that the ROMs of different segments were in good agreement with those experimental measurements under all loading conditions [24-26] (**Figure 4**). Therefore, the three intact models were included for further biomechanical analysis.

Range of motion

In general, all posterior fixation techniques induced a significant decrease in the ROM at the fusion segment with respect to the intact configuration. Among the four implanted models, the highest ROM at the L4-5 level was found for the UCBT configuration, followed by CBT, UCBT-TFS, and TT (**Figure 5**). Compared with the ROM in TT, the ROMs in UCBT markedly increased by 31%, 55%, 116%, 170%, 55%, and 62% in flexion, extension, left bending, right bending, left rotation, and right rotation, respectively. Although the mean value of CBT was slightly higher in lateral bending than that of TT and UCBT-TFS, the three instruments showed comparable stability in other directions. The differences in the ROM among the three implanted models were less than 0.2 degrees.

Stress of cages

In terms of the maximal von Mises stress of the cages, the highest mean value was observed in the UCBT models in each direction, especially in lateral bending and axial rotation (compared to the TT models, increased by 148%, 105%, 55%, and 73% in left bending, right bending, left rotation, and right rotation, respectively). CBT resulted in a similar cage stress to UCBT-TFS, which was higher than the stress of TT in lateral bending and axial rotation. Generally, the TT models still resulted in the lowest stress at the cage surface (average 47 MPa, 15 MPa, 26 MPa, 27 MPa, 45 MPa, and 34 MPa in flexion, extension, left bending, right bending, left rotation, and right rotation, respectively) (**Figure 6**).

The stress of the posterior fixations

A similar change in maximal von Mises stress in the posterior fixations was observed: the highest stress of the instruments was found in the

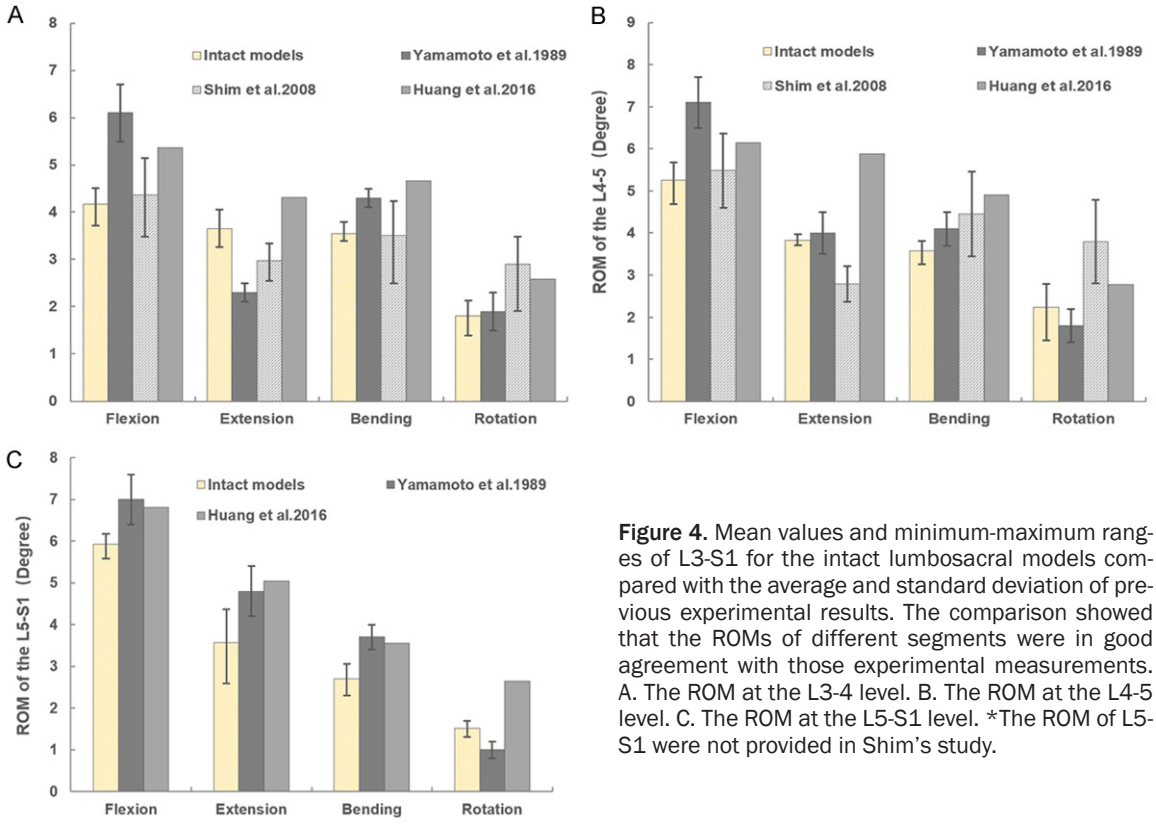

Figure 4. Mean values and minimum-maximum ranges of L3-S1 for the intact lumbosacral models compared with the average and standard deviation of previous experimental results. The comparison showed that the ROMs of different segments were in good agreement with those experimental measurements. A. The ROM at the L3-4 level. B. The ROM at the L4-5 level. C. The ROM at the L5-S1 level. *The ROM of L5-S1 were not provided in Shim's study.

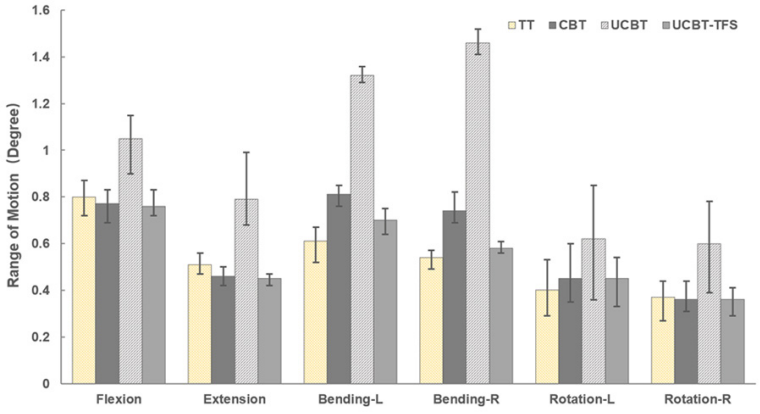

Figure 5. Mean values and minimum-maximum ranges of ROMs at the fixation segment in four implanted models. The highest ROM at the surgical level was found for the UCBT configuration, followed by CBT, UCBT-TFS, and TT.

UCBT models, while TT demonstrated a significant decrease in the stress in each direction (**Figure 7**). The maximum peak von Mises stress in UCBT was observed during flexion, left rotation, and right rotation (average 306, 326, and 292 MPa, respectively). A typical peak von Mises stress of UCBT is shown in **Figure 8**. Finally, UCBT-TFS generally resulted in less stress than CBT but resulted in consistently higher stress than TT under all loading conditions (compared to the TT models, increased by 22%, 6%, 64%, 53%, 45% and 66% in flexion, extension, left bending, right bending, left rotation, and right rotation, respectively).

Discussion

Multiple studies have confirmed that three-column stabilization of the spine can be effectively achieved by pedicle screw fixation. However, despite the advantage of biomechanical stability using pedicle screws, screw loosening and breakage are common complications in patients with osteoporosis. Screws with different trajectories have been developed to improve the holding strength in the vertebral body. From a biomechanical point of view, the forces of the transverse process, lamina, and

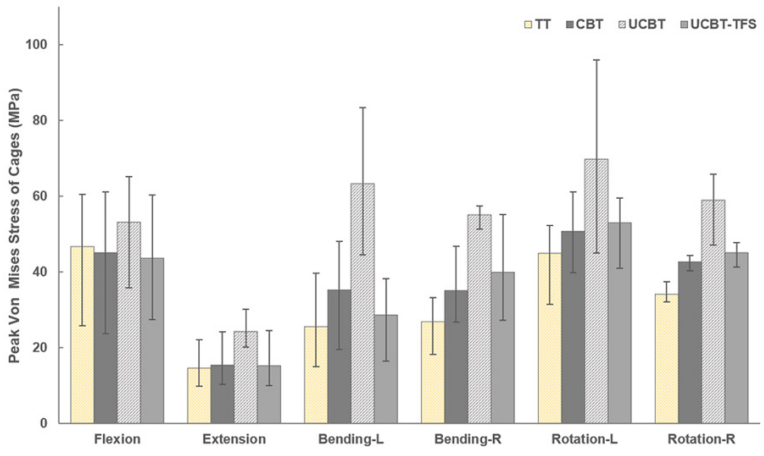

Figure 6. Mean values and minimum-maximum ranges of the peak von Mises stress in the cages in four implanted models. Generally, the TT models still resulted in the lowest stress at the cage surface.

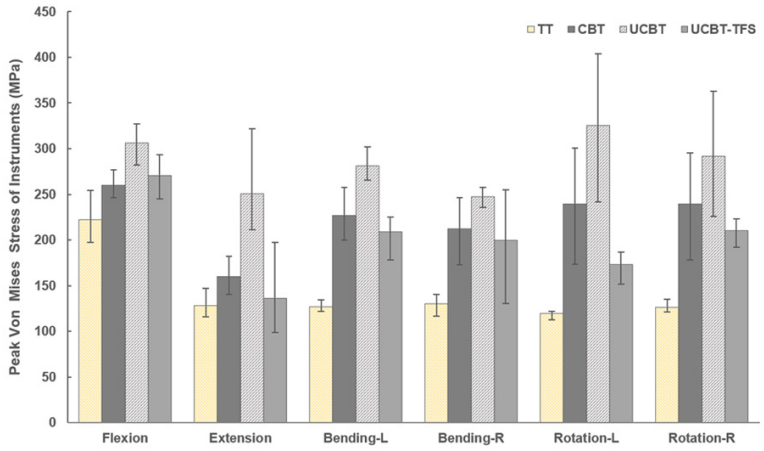

Figure 7. Mean values and minimum-maximum ranges of the peak von Mises stress in posterior fixations in four implanted models. The highest stress of the instruments was found in the UCBT models, while TT demonstrated a significant decrease in the stress in each direction.

facet joint transmit and converge at the pedicle, namely, as the "force nucleus" of the vertebral body [27]. CBT screws obtain good fixation strength by maximizing thread contact with the cortical bone in the "force nucleus", including the dorsal cortical bone at the insertion, the medially oriented posterior pedicle wall, the laterally oriented anterior pedicle wall, and the curvature of the vertebral body wall [7]. Therefore, the CBT technique offers superior fixation strength over the TT technique in some conditions.

Although there was a slightly higher ROM in lateral bending, this study showed that bilateral CBT demonstrated similar fixation strength to TT. This result was consistent with several previous biomechanical studies by Matsukawa et al. [28, 29]. The authors found that CBT screws demonstrated greater vertebral stability in flexion-extension and lower stability in lateral bending and rotation than TT screws in the normal lumbar spine, while they demonstrated statistically lower fixation strength in the spondylolytic spine. This may be related to the shorter lever arm and smaller spacing of the CBT construct. In terms of internal fixation stress, the maximum stress of CBT was also higher than that of TT, especially in lateral bending and rotation (78%, 63%, 101%, and 89% in left bending, right bending, left rotation, and right rotation, respectively). This may be due to the smaller CBT screws being extensively surrounded by hard cortical bone. Thus, we suggest TT rather than CBT for patients with obesity, spondylolytic vertebrae, and unilateral/bilateral facetectomy to decrease the risk of screw loosening.

Some biomechanical studies and clinical reports have revealed that unilateral pedicle screw techniques can provide similar biomechanical stability [30, 31] and fusion rates [32, 33] to bilateral pedicle screw fixation. However, in terms of UCBT, the ROM, cage stress, and instrument stress were significantly higher than those of TT, which is the gold standard fixation for lumbosacral fusion in the treatment of various spinal diseases. This result indicates that UCBT may make the fusion segment very unstable, especially in lateral bending. In addition, UCBT may also increase the risk of cage subsidence, screw loosening, and nonunion. Therefore, UCBT is less optimal for stabilizing cases of TLIF due to the low fixation strength and large instrument stress.

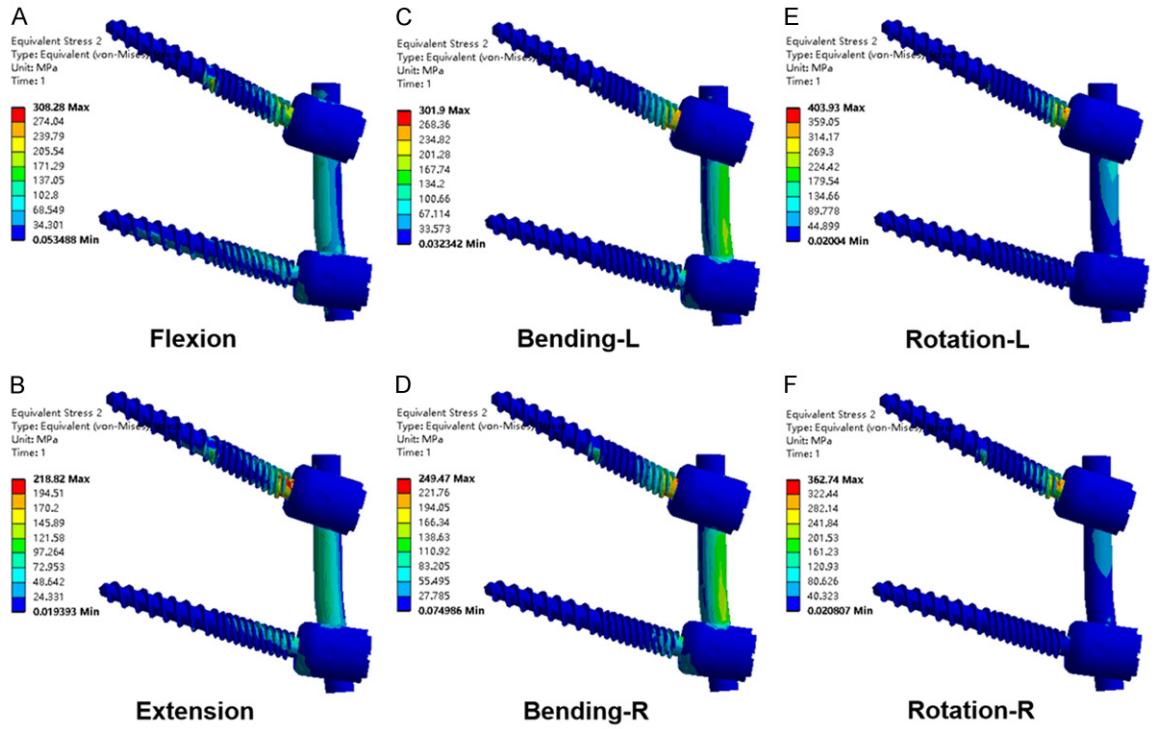

Figure 8. Typical peak von Mises stress of unilateral cortical bone trajectory screw fixation (UCBT) showed that maximum stress was observed during flexion and rotation.

The size of translaminar facet screws (TFS) (3.5 mm diameter and 45 mm length) is similar to that of CBT screws (5 mm diameter and 35 mm length), and both screws pass through the lamina and maximize thread contact with the stiff cortical bone. In addition, the fixed facets significantly reduce motion in flexion, extension, and axial rotation but have less impact in lateral flexion [18]. Translaminar facet screws have shown good fixation strength and are often applied with unilateral pedicle screw fixation [34, 35]. Thus, we assume that the combined fixation of UCBT and TFS can preserve the limited paraspinal muscle dissection of UCBT fixation and overcome the limitations of reduced stability. The data of this study also recommend that a hybrid fixation of UCBT with TFS is a better choice to reduce invasiveness and provide sufficient stability. However, it should be noted that the stress of UCBT-TFS screws is higher than that of TT screws in lateral bending and rotation, which means that patients with UCBT-TFS should be evaluated for their body mass index and postoperative activity.

Some limitations should be mentioned in this computational study. First, as a computer simulation biomechanical experiment, it has connatural drawbacks, such as exclusions of the difference of soft-tissue dissections among four fixations, the effect of different weights, and the complex movements of the spine. Second, the nonlinear characteristics of the ligaments were simplified, and the effects of fat and skin were excluded. Furthermore, our biomechanical study only focused on single-level conditions and single-interbody cage TLIF, and the biomechanical results of these techniques at 2 levels or with other lumbar fusion techniques have not been obtained.

In conclusion, among the four different fixation techniques, TT offered the highest fixation strength and lowest implant stress, followed by UCBT-TFS and CBT, while UCBT was the least stable and resulted in increased stress of the screws and cages. UCBT-TFS improved biomechanical stability and appeared to be a less invasive alternative in well-selected patients with single-level TLIF.

Acknowledgements

This study was funded by The First Affiliated Hospital of Guangzhou University of Chinese

Medicine innovation and strength project (2019IIT32).

Disclosure of conflict of interest

None.

Address correspondence to: Dr. Shun-Cong Zhang, Spine Surgery Department, The First Affiliated Hospital of Guangzhou University of Chinese Medicine, 12 Airport Road, Baiyun District, Guangzhou 510405, Guangdong, China. Tel: +86-13602765101; E-mail: 18122436960@163.com

References

[1] Deyo RA. Fusion surgery for lumbar degenerative disc disease: still more questions than answers. Spine J 2015; 15: 272-274.

[2] BOUCHER HH. A method of spinal fusion. J Bone Joint Surg Br 1959; 41-B: 248-259.

[3] Guo HZ, Tang YC, Li YX, Yuan K, Guo DQ, Mo GY, Luo PJ, Zhou TP, Zhang SC and Liang D. The effect and safety of polymethylmethacrylate-augmented sacral pedicle screws applied in osteoporotic spine with lumbosacral degenerative disease: a 2-year follow-up of 25 patients. World Neurosurg 2019; 121: e404-e410.

[4] Lee KY, Lee JH, Kang KC, Shin SJ, Shin WJ, Im SK and Park JH. Strategy for obtaining solid fusion at L5-S1 in adult spinal deformity: risk factor analysis for nonunion at L5-S1. J Neurosurg Spine 2020; 1-9.

[5] Leng J, Han G, Zeng Y, Chen Z and Li W. The effect of paraspinal muscle degeneration on distal pedicle screw loosening following corrective surgery for degenerative lumbar scoliosis. Spine (Phila Pa 1976) 2020; 45: 590-598.

[6] Santoni BG, Hynes RA, McGilvray KC, Rodriguez-Canessa G, Lyons AS, Henson MA, Womack WJ and Puttlitz CM. Cortical bone trajectory for lumbar pedicle screws. Spine J 2009; 9: 366-373.

[7] Matsukawa K, Yato Y, Kato T, Imabayashi H, Asazuma T and Nemoto K. In vivo analysis of insertional torque during pedicle screwing using cortical bone trajectory technique. Spine (Phila Pa 1976) 2014; 39: E240-245.

[8] Kotheeranurak V, Lin GX, Mahatthanatrakul A and Kim JS. Endoscope-assisted anterior lumbar interbody fusion with computed tomography-guided, image-navigated unilateral cortical bone trajectory screw fixation in managing adjacent segment disease in L5/S1: technical note. World Neurosurg 2019; 122: 469-473.

[9] Wang Md K, Jiang PhD C, Wang PhD L, Wang Md H and Niu PhD W. The biomechanical influence of anterior vertebral body osteophytes on the lumbar spine: a finite element study. Spine J 2018; 18: 2288-2296.

[10] Xu H, Ju W, Xu N, Zhang X, Zhu X, Zhu L, Qian X, Wen F, Wu W and Jiang F. Biomechanical comparison of transforaminal lumbar interbody fusion with 1 or 2 cages by finite-element analysis. Neurosurgery 2013; 73: ons198-205.

[11] Lu T and Lu Y. Comparison of biomechanical performance among posterolateral fusion and transforaminal, extreme, and oblique lumbar interbody fusion: a finite element analysis. World Neurosurg 2019; 129: e890-e899.

[12] Fantigrossi A, Galbusera F, Raimondi MT, Sassi M and Fornari M. Biomechanical analysis of cages for posterior lumbar interbody fusion. Med Eng Phys 2007; 29: 101-109.

[13] Wang TM and Shih C. Morphometric variations of the lumbar vertebrae between Chinese and Indian adults. Acta Anat (Basel) 1992; 144: 23-29.

[14] Bach K, Ford J, Foley R, Januszewski J, Murtagh R, Decker S and Uribe JS. Morphometric analysis of lumbar intervertebral disc height: an imaging study. World Neurosurg 2018; 124: E106-E118.

[15] Pan C, Wang G and Sun J. Correlation between the apex of lumbar lordosis and pelvic incidence in asymptomatic adult. Eur Spine J 2020; 29: 420-427.

[16] Li WS, Sun ZR and Chen ZQ. Radiographic analysis of spinopelvic sagittal alignment and prediction of lumbar lordosis in Chinese asymptomatic subjects. Global Spine J 2015; 5.

[17] Sakaura H, Miwa T, Yamashita T, Kuroda Y and Ohwada T. Cortical bone trajectory screw fixation versus traditional pedicle screw fixation for 2-level posterior lumbar interbody fusion: comparison of surgical outcomes for 2-level degenerative lumbar spondylolisthesis. J Neurosurg Spine 2018; 28: 57-62.

[18] Liu F, Feng Z, Liu T, Fei Q, Jiang C, Li Y, Jiang X and Dong J. A biomechanical comparison of 3 different posterior fixation techniques for 2-level lumbar spinal disorders. J Neurosurg Spine 2016; 24: 375-380.

[19] Reis MT, Reyes PM, Bse, Altun I, Newcomb AG, Singh V, Chang SW, Kelly BP and Crawford NR. Biomechanical evaluation of lateral lumbar interbody fusion with secondary augmentation. J Neurosurg Spine 2016; 25: 720-726.

[20] Guo HZ, Tang YC, Guo DQ, Luo PJ, Li YX, Mo GY, Ma YH, Peng JC, Liang D and Zhang SC. Stability evaluation of oblique lumbar interbody fusion constructs with various fixation options: a finite element analysis based on three-dimensional scanning models. World Neurosurg 2020; 138: E530-E538.

[21] La Barbera L, Cianfoni A, Ferrari A, Distefano D, Bonaldi G and Villa T. Stent-screw assisted internal fixation of osteoporotic vertebrae: a comparative finite element analysis on SAIF technique. Front Bioeng Biotechnol 2019; 7: 291.
[22] Jones AC and Wilcox RK. Finite element analysis of the spine: towards a framework of verification, validation and sensitivity analysis. Med Eng Phys 2008; 30: 1287-1304.
[23] Wang T, Zhao Y, Cai Z, Wang W, Xia Y, Zheng G, Liang Y and Wang Y. Effect of osteoporosis on internal fixation after spinal osteotomy: a finite element analysis. Clin Biomech (Bristol, Avon) 2019; 69: 178-183.
[24] Yamamoto I, Panjabi MM, Crisco T and Oxland T. Three-dimensional movements of the whole lumbar spine and lumbosacral joint. Spine (Phila Pa 1976) 1989; 14: 1256-1260.
[25] Shim CS, Park SW, Lee SH, Lim TJ, Chun K and Kim DH. Biomechanical evaluation of an interspinous stabilizing device, locker. Spine (Phila Pa 1976) 2008; 33: E820-827.
[26] Huang YP, Du CF, Cheng CK, Zhong ZC, Chen XW, Wu G, Li ZC, Ye JD, Lin JH and Wang LZ. Preserving posterior complex can prevent adjacent segment disease following posterior lumbar interbody fusion surgeries: a finite element analysis. PLoS One 2016; 11: e0166452.
[27] Steffee AD, Biscup RS and Sitkowski DJ. Segmental spine plates with pedicle screw fixation. A new internal fixation device for disorders of the lumbar and thoracolumbar spine. Clin Orthop Relat Res 1986: 45-53.
[28] Matsukawa K, Yato Y, Imabayashi H, Hosogane N, Asazuma T and Nemoto K. Biomechanical evaluation of the fixation strength of lumbar pedicle screws using cortical bone trajectory: a finite element study. J Neurosurg Spine 2015; 23: 471-478.
[29] Matsukawa K, Yato Y, Imabayashi H, Hosogane N, Asazuma T and Chiba K. Biomechanical evaluation of lumbar pedicle screws in spondylolytic vertebrae: comparison of fixation strength between the traditional trajectory and a cortical bone trajectory. J Neurosurg Spine 2016; 24: 910-915.
[30] Chen HH, Cheung HH, Wang WK, Li A and Li KC. Biomechanical analysis of unilateral fixation with interbody cages. Spine (Phila Pa 1976) 2005; 30: E92-96.
[31] Li J, Wang W, Zuo R and Zhou Y. Biomechanical stability before and after graft fusion with unilateral and bilateral pedicle screw fixation: finite element study. World Neurosurg 2019; 123: e228-234.
[32] Zhao Y, Yang S and Ding W. Unilateral versus bilateral pedicle screw fixation in lumbar fusion: a systematic review of overlapping meta-analyses. PLoS One 2019; 14: e0226848.
[33] Wen J, Shi C, Yu L, Wang S, Xi Y and Ye X. Unilateral versus bilateral percutaneous pedicle screw fixation in oblique lumbar interbody fusion. World Neurosurg 2020; 134: e920-e927.
[34] Zeng ZY, Wu P, Yan WF, Song YX, Zhang JQ, Tang HC, Song GH, Han JF and Fan SW. Mixed fixation and interbody fusion for treatment single-segment lower lumbar vertebral disease: midterm follow-up results. Orthop Surg 2015; 7: 324-332.
[35] Huang P, Wang Y, Xu J, Xiao B, Liu J, Che L and Mao K. Minimally invasive unilateral pedicle screws and a translaminar facet screw fixation and interbody fusion for treatment of single-segment lower lumbar vertebral disease: surgical technique and preliminary clinical results. J Orthop Surg Res 2017; 12: 117.